Journal of the Energy Institute 88 (2015) 43–52

Contents lists available at ScienceDirect

Journal of the Energy Institute

journal homepage: http://www.journals.elsevier.com/journal-of-the-energy-institute

Comparison of steam injected diesel engine and Miller cycled diesel engine by using two zone combustion model

Guven Gonca [a,*], Bahri Sahin [a], Yasin Ust [a], Adnan Parlak [b], Aykut Safa [a]

[a] Department of Naval Architecture and Marine Engineering, Yildiz Technical University, 34349 Istanbul, Turkey
[b] Department of Marine Engineering Operations, Yildiz Technical University, 34349 Istanbul, Turkey

ARTICLE INFO

Article history:
Received 12 November 2012
Accepted 11 March 2014
Available online 26 April 2014

Keywords:
Miller cycle
Engine performance
Diesel engine
Steam injection
NO_x

ABSTRACT

Emissions, especially NO_x, released from diesel engines must be decreased to limit values described by the regulations because emissions have many bad effects on the environment. One of the known methods for reduction NO_x emissions is to apply Miller Cycle to a diesel engine. In this study, Miller cycle is carried out by lowering the compression ratio according to the expansion ratio with closing the intake valve 30° crank angle later from the BDC (Bottom Dead Center) compared to standard diesel engine. Another method used is steam injection into diesel engine to decrease NO_x emissions. And also, this method could be used to improve the performance and efficiency. Because of these positive effects, Miller cycle and steam injection methods could be implemented into diesel engines together. In this paper, Miller cycled diesel engine with steam injection has been modeled by using zero-dimensional two-zone combustion model. The obtained results have been compared with conventional diesel engine, Miller Cycled diesel engine and steam injected diesel engine in terms of performance and NO emissions. In the results, Miller Cycled diesel engine with steam injection is more efficient at low and medium engine speeds and has less NO emissions than conventional diesel engine, steam injected diesel engine and Miller Cycled diesel engine in all conditions.

1. Introduction

Diesel engines have a prominent place in the modern life. Diesel engines must be designed by considering environmental reasons as other engines using global fuel resources. Because of environmental restrictions, particularly the reduction of NO_x emissions is needed.

One of the known methods to decrease NO_x emissions is to apply Miller cycle to the diesel engine. Applying Miller cycle to the diesel engine could reduce the NO_x emissions released from the diesel engine was shown by Wang et al. [1] experimentally. Mikalsen et al. [2] studied on effects of using Miller Cycle on natural gas engine by comparing with Otto cycle. In the study, the fuel efficiency of natural gas engine is increased but at the cost of a less powerful engine. Wang et al. [3] applied the Miller Cycle to a petrol engine to lessen NO_x emissions by closing intake valve lately. In their study a comparison of the characteristics of Miller cycle with Otto cycle and thermodynamic analysis of the Miller cycle is presented. The compression pressure and temperature were decreased in the cylinder at the end of the compression stroke hence; NO_x formation and combustion temperature diminish as well. Ge et al. [4] studied on the effects of friction loss and heat transfer loss on the performance of an air standard Miller cycle by using finite-time thermodynamics. In the another study, Ge et al. [5] analyzed and compared the Reciprocating heat-engine cycles by using finite-time thermodynamics and also, it is showed that the performance of the Miller cycle by using numerical examples. Al-Sarkhi et al. [6] analyzed an air standard Miller cycle in terms of thermal efficiency, compression and expansion ratios. In this study, it is expressed that the effect of the temperature-dependent specific heat of the working fluid on the irreversible Miller cycle was essential. Lin and Hou [7] conducted an analysis of an air-standard Miller cycle taking into account of heat loss as a percentage of fuel's energy, friction and variable specific heats of working fluid under the restriction of peak temperature of the cycle. They compared the Miller cycle with Otto cycle in terms of power output and efficiency and showed that the

* Corresponding author. Tel.: +90 212 3832950; fax: +90 212 236 41 65.
E-mail addresses: ggonca@yildiz.edu.tr (G. Gonca), bsahin@yildiz.edu.tr (B. Sahin), yust@yildiz.edu.tr (Y. Ust), aparlak@yildiz.edu.tr (A. Parlak), asafa@yildiz.edu.tr (A. Safa).

http://dx.doi.org/10.1016/j.joei.2014.04.007
1743-9671/

Nomenclature

A	heat transfer area (cm^2)
C_v	constant volume specific heat(J g^{-1} K^{-1})
C_p	constant pressure specific heat(J g^{-1} K^{-1})
C	blow by coefficient
B	bore (cm)
F	fuel-air ratio
h	specific enthalpy (J g^{-1})
h_{tr}	heat transfer coefficient (W m^{-2} K^{-1}) of burned and unburned zone
H	enthalpy (J g^{-1})
H_u	low heat value (J g^{-1})
m	mass (g)
$\dot{m}$	time-dependent mass rate (g s^{-1})
M	molecular weight
n	injection constant
P	pressure (bar)
R	gas constant (J g^{-1} K^{-1})
NR	revolution per minute
NY	total mole number
Q	loss heat passed through the cylinder wall (J)
$\dot{Q}$	rate of heat transfer (W)
RGF	residual gas fraction
s	specific entropy (J g^{-1} K^{-1})
S	stroke (cm)
$\bar{S}_p$	mean piston velocity (m s^{-1})
T	temperature (K)
u	specific internal energy (J g^{-1})
v	specific volume (cm^3 g^{-1})
V	volume (cm^3)
W	work output (J)
x	burn fraction
$\dot{x}_i$	fraction rate of the total injected fuel mass
$Y_{\%}$	ratio of the steam mass to the fuel mass

Greek letters

ε	ratio of half stroke to rod length
ϕ	equivalence ratio
Γ(n)	gamma function
θ	crank angle (degree)
τ	time (ms)
ω	angular velocity (rad s^{-1})

Subscripts

0	at the beginning of compression for steam injected condition
1	at the beginning of compression for standard condition
a	air
b	burned zone
cyl	cylinder
di	injection duration parameter
dif	diffusive combustion phase
f	fuel
fi	injected fuel
id	ignition delay(ms)
l	leak, loss
pre	premixed combustion phase
r	reference
si	start of fuel injection (degree)
st	stoichiometric
ste	steam
tfmep	total friction mean effective pressure
u	unburned zone
w	cylinder walls

performance of the Miller cycle was better than Otto cycle. Al-Sarkhi et al. [8] conducted a research on a Miller engine in terms of different specific heat models. Wu et al. [9] performed an analysis of supercharged Miller Cycled Otto engine. According to the study, they expressed that the Miller Cycle Otto engine has more work output and could have less engine knock problem. Kesgin [10], applied the Miller cycle to a V20 engine. The Miller cycle was analyzed experimentally and computationally. The efficiency of the engine was increased and NO_x emissions were kept under the limit.

Uzuneanu and Panait [11] indicated that the thermal efficiency of a supercharged Miller Cycle depends on various engine parameters. Zhao and Chen [12] performed a study on an irreversible Miller Cycle model considering some irreversibilities in the compression, expansion, finite time processes and heat loss through the cylinder wall. In their study, an optimization was carried out with respect to the pressure ratios. The optimum criteria of the power output, efficiency and pressure ratio were defined. Gonca et al. [13,14] applied the miller cycle to the diesel engine by using two-zone combustion model and compared the results of conventional diesel and miller cycled diesel engine. Gonca et al. [15] conducted a study on a diesel engine running with miller cycle by using single-zone combustion model. Gonca et al. [16] performed a numerical analysis based on the maximum power output and maximum thermal efficiency criteria for an air-standard irreversible dual miller cycle with late inlate valve closing version.

In many studies, it is expressed that maximum combustion temperature and NO_x emissions were decreased in the case of using diesel fuel with water in the engine [17–22]. Bedford et al. [23] studied on the effects of in-cylinder water injection on a direct injection (DI) Diesel engine by using a computational fluid dynamics (CFD) program. In their study, NO_x and smoke formation rates were reduced. Armas et al. [24] conducted a study on the effect of water–oil emulsions on the engine performance and pollutant emissions. Results presented that the water emulsification had a potential to improve the brake efficiency and decrease the formation of emissions. Abu-Zaid [25], conducted a study on using water-diesel emulsions in diesel engine to investigate the effect on the engine performance and gases exhaust temperature. In his study, results indicated that the addition of water in form of emulsion increases the engine torque, power and brake thermal efficiency and decreases brake specific fuel consumption and exhaust gas temperature. Sarvi et al. [26] investigated the influence of direct water injection (DWI) and Common Rail (CR) technology on emissions released from a multivariable large-scale medium-speed diesel engine. They showed that Combining CR with DWI resulted in lower NO_x and HC emissions but slightly higher CO and smoke emissions. Ayhan [27] investigated the effect of steam injection on the reduction of NO_x emissions released from a diesel engine with direct injection system. Parlak et al. [28] and Kokkulunk et al. [29] applied the steam injection technique to a diesel engine and Cesur et al. [30] applied this method to a gasoline engine. Gonca [31] examined the effects of steam injection on a diesel engine running with ethanol-diesel blend. Parlak et al. [32] investigated the influences of the steam injection on a diesel engine fueled with tobacco seed oil methyl ester. Gonca et al. [33] carried

out a theoretical analysis based on thermodynamics to determine the optimum steam temperatures and mass ratios for turbocharged internal combustion engines. In these studies, the authors demonstrated that steam injection reduced NO_x emissions and increased torque, effective power and effective efficiency considerably.

In this study, apart from the given above studies, Late Inlet Valve Closing (LIVC) Miller Cycled Diesel engine with steam injection has been modeled by using zero-dimensional two-zone combustion model and the results are compared with those of conventional Diesel engine, Miller Cycled Diesel engine and diesel engine with steam injection in terms of performance and NO emissions, respectively.

2. Theoretical model

Thermodynamic simulation of fuel injected engine is performed by using two-zone combustion model to calculate emissions, efficiency and power. The burned and unburned gas regions are divided by region border. The fuel injected into the combustion chamber reacts with the air in the unburned region and becomes a part of the burnt gas region by combustion. In the cylinder, the equation of the energy conservation in differential form could be expressed as:

$$m\frac{du}{d\theta}+u\frac{dm}{d\theta}=-\frac{dQ_b}{d\theta}-\frac{dQ_u}{d\theta}-P\frac{dV}{d\theta}+\frac{dm_{fi}}{d\theta}h_{fi}-\frac{dm_l}{d\theta}h_l \tag{1}$$

Where m_l is leak mass and m_{fi} is mass of injected fuel; h_{fi} and h_l are enthalpies of fuel injected and leak mass respectively. The first term of the left side of the equation is the internal energy rate and the second term is the mass rate depending on crank angle. The heat transfers from burned and unburned zone are expressed, respectively as:

$$\dot{Q}_b = h_{tr}A_bT_{bw} \tag{2}$$

$$\dot{Q}_u = h_{tr}A_uT_{uw} \tag{3}$$

where $T_{\mathrm{uw}}=T_u-T_w$ and $T_{\mathrm{bw}}=T_b-T_w$, h_{tr} is heat transfer coefficient of burned and unburned gas zones, A_b and A_u are the areas of burned and unburned gas inside the cylinder which are in contact with the cylinder walls and T_b, T_u and T_w are the temperatures of the burned gas zone, unburned gas zone and cylinder walls [34]. The change of stroke volume depending on crank angle is:

$$\frac{dV}{d\theta}=\frac{\pi}{8}B^2\,S\sin\theta\left[1+\varepsilon\,\frac{\cos\theta}{(1-\varepsilon^2\sin^2\theta)^{\frac{1}{2}}}\right] \tag{4}$$

In order to solve the differential equations, the following expressions are used in the model. Internal energy:

$$\frac{du}{d\theta}=C_p-\frac{Pv}{T}\left(\frac{\partial\ln v}{\partial\ln T}\right)_P\frac{dT}{d\theta}-v\left[\frac{\partial\ln v}{\partial\ln T}+\frac{\partial\ln v}{\partial\ln P}\right]_T\frac{dP}{d\theta}+\frac{\partial u}{\partial\phi}\frac{d\phi}{d\theta} \tag{5}$$

The burned gas leaking through the rings:

$$\frac{dm_l}{d\theta}=\frac{Cm}{\omega} \tag{6}$$

where C and ω are blow by coefficient and angular velocity, respectively. The mass balance inside the cylinder can be expressed as:

$$m = m_a+m_{fi} \tag{7}$$

where m_a and m_{fi} are the masses of the air and injected fuel respectively. If the Eq. (7) is written in differential form, it becomes:

$$\frac{dm}{d\theta}=\frac{dm_a}{d\theta}+\frac{dm_{fi}}{d\theta} \tag{8}$$

The air and injected fuel rates changing with crank angle within the cylinder are expressed respectively as:

$$\frac{dm_a}{d\theta}=\frac{-\dot{m}_l/\omega}{1+\phi F_{st}}=\frac{-Cm_a}{\omega} \tag{9}$$

$$\frac{dm_{fi}}{d\theta}=\frac{1}{\omega}\left(\dot{m}_{fi}-\frac{\dot{m}_l\phi F_{st}}{1+\phi F_{st}}\right)=\frac{\dot{m}_{fi}-Cm_{fi}}{\omega} \tag{10}$$

where $\dot{m}_l$, φ and F_s are the time-dependent gas leak rate, the equivalence ratio and the stoichiometric fuel-air ratio by mass, respectively. $\dot{m}_{\mathrm{fi}}$ is the time-dependent fuel injected rate and can be expressed as:

$$\dot{m}_{fi} = \dot{x}_i\,m_{fi} \tag{11}$$

where m_{fi} and$\dot{x}_i$ are the total mass of the fuel to be injected and fraction rate of the total injected fuel mass respectively, which can be given as:

$$m_{fi} = \phi F_{st}(1 - RGF)m_a \tag{12}$$

$$\dot{x}_i = \frac{\omega}{\theta_{di}\Gamma(n)}\left(\frac{\theta - \theta_{si}}{\theta_{di}}\right)^{n-1} \exp\left[\frac{-(\theta - \theta_{si})}{\theta_{di}}\right] \tag{13}$$

where $\Gamma(n)$ is the gamma function [34], θ_{di} is a parameter of injection duration and θ_{si} is the start of fuel injection. The gamma function is derived as:

$$\ln\Gamma(n) = \left(n - \frac{1}{2}\right)\ln(n) - n + \frac{1}{2}\ln(2\pi) + \frac{1}{12n} - \frac{1}{360n^3} + \frac{1}{1260n^5} - \frac{1}{1680n^7} \tag{14}$$

The values of n could be taken for the diesel engine with open chamber as $1 \le n \le 2$ and for close chamber as $3 \le n \le 5$ but exact value is dependent on fuel used and engine design [34]. Differential equation systems used in the calculation of the processes that consist during the period from the beginning of the compression to the end of the expansion process are given in Eqs. (15)–(20) [14,31,35].

The time (crank angle)-dependent expressions of pressure, burned and unburned gas temperatures, work, heat leak and heat loss are given respectively as:

$$\frac{dP}{d\theta} = \frac{\begin{array}{l}\frac{C}{\omega}\left(\frac{V}{m} + \frac{\vartheta_1}{C_{p,b}T_b}\left(\left(x^2 - x\right)(h_b - h_u)\right)\right) + \frac{h_{tr}}{\omega m}A_{cyl}\left(\begin{array}{l}\sqrt{x}\ \frac{\vartheta_1}{C_{p,b}T_b}T_{bw} + \\ (1-\sqrt{x})T_{uw}\frac{\vartheta_2}{C_{p,u}T_u}\end{array}\right) + \left(\begin{array}{l}\frac{\vartheta_1}{C_{p,b}T_b}(h_b - h_u) - \\ (v_b - v_u)\end{array}\right)\frac{dx}{d\theta} + \frac{1}{m}\frac{dV}{d\theta} + \\ \left(\begin{array}{l}\frac{\vartheta_1}{m\ C_{p,b}T_b}\left(\begin{array}{l}x\ h_b - \\ (1-x)h_u\end{array}\right) - \\ H_u - \frac{V}{m^2}\end{array}\right)\frac{dm_{fi}}{d\theta} + (1-x)\left(\begin{array}{l}\frac{\vartheta_1}{C_{p,b}T_b}\left(\begin{array}{l}-T_u\frac{ds_u}{d\theta} + \\ P\frac{dv_u}{d\theta} + \frac{du_u}{d\theta}\end{array}\right) - \\ \frac{dv_u}{d\theta} + \frac{\vartheta_2}{C_{p,u}}\frac{ds_u}{d\theta}\end{array}\right)\frac{d\phi}{d\theta} + x\left(\begin{array}{l}\frac{\vartheta_1}{C_{p,b}T_b}\left(P\frac{dv_b}{d\theta} + \frac{du_b}{d\theta}\right) - \\ \frac{dv_b}{d\theta}\end{array}\right)\frac{d\phi}{d\theta}\end{array}}{x\left(\frac{\vartheta_1}{C_{p,b}T_b} + \frac{\vartheta_3}{P}\right) + (1-x)\left(\frac{\vartheta_2^2}{C_{p,u}T_u} + \frac{\vartheta_4}{P}\right)} \tag{15}$$

Where x, H_u, A_{cyl} are the burning fraction, lower heating value of fuel and heat transfer area of the cylinder. $C_{p,b}$,$C_{p,u}$;v_b,v_u; s_b,s_u;h_b,h_u are specific heat at constant pressure, specific volume, specific entropy and specific enthalpy for the burned and unburned zones respectively.

$$\vartheta_1 = \frac{\partial In\ v_b}{\partial In\ T_b}v_b, \quad \vartheta_2 = \frac{\partial In\ v_u}{\partial In\ T_u}v_u$$

$$\vartheta_3 = \frac{\partial In\ v_b}{\partial In\ T_b}v_b, \quad \vartheta_4 = \frac{\partial In\ v_u}{\partial In\ T_u}v_u$$

$$\frac{dT_b}{d\theta} = \frac{1}{C_{p,b}}\left(-\frac{h_{tr}}{\omega\ m}A_{cyl}\frac{1}{\sqrt{x}}T_{bw} + \vartheta_1\frac{dP}{d\theta}\right) \tag{16}$$

$$\frac{dT_u}{d\theta} = -\frac{h_{tr}}{\omega m C_{pu}}A_{cyl}\frac{T_{uw}}{1+\sqrt{x}} + \frac{\vartheta_2}{C_{pu}}\frac{dP}{d\theta} - \frac{\partial s_b}{\partial\phi}\frac{d\phi}{d\theta}\frac{1}{C_{pb}} \tag{17}$$

$$\frac{dW}{d\theta} = -P\frac{dV}{d\theta} \tag{18}$$

$$\frac{dH_l}{d\theta} = \frac{Cm}{\omega}\left[\left(1 - x^2\right)h_u + x^2 h_b\right] \tag{19}$$

$$\frac{dQ_l}{d\theta} = \frac{h_{tr}}{\omega}A_{cyl}\left[\sqrt{x}T_{bw} + (1-\sqrt{x})T_{uw}\right] \tag{20}$$

Hohenberg [36] gives the coefficient of the heat transfer (h_{tr}) as below:

$$h_{tr} = C_1 V^{-0.06}P^{0.8}(xT_b + (1-x)T_u)^{-0.4}\left(\overline{S}_p + C_2\right)^{0.8} \tag{21}$$

where $\overline{S}_p$ is mean piston velocity in meters per second, $C_1 = 130$ and $C_2 = 1.4$ respectively. Sitkei [37] correlation is used to calculate ignition delay and it is written as following:

$$\tau_{id} = 0.5 + 0.1332\,P^{-0.7}e^{\frac{3.92782}{T}} + 4.637\,P^{-1.8}e^{\frac{3.92782}{T}} \tag{22}$$

where P and T are average temperature and pressure of during the ignition delay. Dual Wiebe function states the burn fraction and x versus crank angle is used to express the heat release from combustion and determined as following [38]

$$x = a_v\left[Q_{pre}\left(1 - e^{-a_v\left(\frac{\theta}{\theta_{pre}}\right)^{(m_{pre}+1)}}\right) + Q_{dif}\left(1 - e^{-a_v\left(\frac{\theta}{\theta_{dif}}\right)^{(m_{dif}+1)}}\right)\right] \tag{23}$$

where Q_{pre} and Q_{dif} are heat release rate of premixed and diffusive combustion. x is 0 at the beginning of the combustion and x becomes 1 at the end of the combustion. It can be rewritten by differentiating with respect to crank angle

$$\frac{dx}{d\theta} = a_v\left[\frac{Q_{pre}}{\theta_{pre}}(m_{pre}+1)\left(\frac{\theta}{\theta_{pre}}\right)^{m_{pre}} e^{-a_v\left(\frac{\theta}{\theta_{pre}}\right)^{(m_{pre}+1)}} + \frac{Q_{dif}}{\theta_{dif}}\left(m_{dif}+1\right)\left(\frac{\theta}{\theta_{dif}}\right)^{m_{dif}} e^{-a_v\left(\frac{\theta}{\theta_{dif}}\right)^{(m_{dif}+1)}}\right] \tag{24}$$

$$\theta = \theta_r - \theta_b \tag{25}$$

where θ_r and θ_b are reference crank angle and start angle of combustion respectively, a_v, m_{pre}, θ_{pre}, m_{dif}, θ_{dif} are Wiebe constants in the premixed and diffusive combustion conditions.

3. Theoretical model of steam injection

NO emissions are calculated by using extended Zeldovich mechanism taking into account 10 combustion products including (CO_2,H_2O,N_2,O_2,CO,H_2,H,O,OH,NO). [15,29–31,39]. In this study the ECP code which is developed by Olikara and Borman [40] is modified by adding steam injection into the reactants. The combustion reaction used in the modified program is given below:

$$\varepsilon\phi\left(C_\alpha H_\beta O_\gamma N_\delta\right) + (0.21O_2 + 0.79N_2) + zH_2O \rightarrow \nu_1 CO_2 + \nu_2 H_2O + \nu_3 N_2 + \nu_4 O_2 + \nu_5 CO + \nu_6 H_2 + \nu_7 H + \nu_8 O + \nu_9 OH + \nu_{10} NO \tag{26}$$

$$\begin{aligned}
&\varepsilon\phi\alpha = (y_1 + y_5)NY\\
&\varepsilon\phi\beta + 2y = (2y_2 + 2y_6 + y_7 + y_9)NY\\
&\varepsilon\phi\gamma + 2\cdot 0,21 + y = \begin{pmatrix} 2y_1 + y_2 + 2y_4 + \\ y_5 + y_8 + y_9 + y_{10}\end{pmatrix}NY\\
&\varepsilon\phi\gamma + 2\cdot 0,79 = (2y_3 + y_{10})NY
\end{aligned} \tag{27}$$

where NY is the total mole number and could be defined as follow:

$$NY = \sum_{i=1}^{10}\nu_i \quad and \quad \sum_{i=1}^{10} y_i - 1 = 0 \tag{28}$$

$$\begin{aligned}
&y_2 + 2y_6 + y_7 + y_9 - (y_1 + y_5)\cdot\frac{\varepsilon\phi\beta + 2z}{\varepsilon\phi\alpha} = 0\\
&2y_1 + y_2 + 2y_4 + y_5 + y_8 + y_9 + y_{10} - \frac{\varepsilon\phi\gamma + 2\cdot 0,21 + z}{\varepsilon\phi\alpha}(y_1 + y_5) = 0\\
&2y_3 + y_{10} - \frac{\varepsilon\phi\gamma + 2\cdot 0,79}{\varepsilon\phi\alpha}(y_1 + y_5) = 0
\end{aligned} \tag{29}$$

The mole fractions of the species could be expressed in terms of y_3, y_4, y_5, y_6.

$$\begin{aligned}
&y_7 = c_1 y_7^{1/2}, \quad y_8 = c_2 y_4^{1/2}, \quad y_9 = c_3 y_4^{1/2} y_6^{1/2},\\
&y_{10} = c_4 y_4^{1/2} y_3^{1/2}, \quad y_2 = c_5 y_4^{1/2} y_6, \quad y_1 = c_6 y_4^{1/2} y_5\\
&c_1 = \frac{K_1}{P^{1/2}}, \quad c_2 = \frac{K_2}{P^{1/2}}, \quad c_3 = K_3\\
&c_4 = K_4, \quad c_5 = K_5 P^{1/2}, \quad c_6 = K_6 P^{1/2}
\end{aligned} \tag{30}$$

where K_i is the equilibrium constant and calculated by using Eq. (31).

$$\log K_i = A\,In\left(\frac{T}{1000}\right) + \left(\frac{B}{T}\right) + C + (DT) + \left(ET^2\right) \tag{31}$$

The A, B, C, D and E constants are taken from JANAF tables [34]. The z constant in the reactants is mole fraction of injected steam and can be calculated as:

$$z = \frac{Y_{\%}\varepsilon\phi M_f}{M_{ste}} \tag{32}$$

where M_f and M_{ste} are molecular weights of the fuel and steam. $Y_{\%}$ is ratio of the steam mass to the fuel mass and defined as:

$$Y_{\%} = \frac{m_{ste}}{m_f} \tag{33}$$

These equations are solved with Newton–Raphson iteration method and results are obtained as in Feguson's study [34]. The charge pressure and temperature at the beginning of the compression stroke of the steam injected cycle are given as: [14,31]

$$\begin{aligned} P_0 &= \frac{m_{ste}\,R_{ste}\,T_{ste} + m_a\,R_a\,T_a}{V} \\ T_0 &= \frac{m_a C_{v,a}\,T_a + m_{ste} C_{v,ste}\,T_{ste}}{m_a C_{v,a} + m_{ste} C_{v,ste}} \end{aligned} \tag{34}$$

where V is the cylinder volume which is changing with respect to crank angle, $C_{v,a}$ and $C_{v,\mathrm{ste}}$ are the specific heat at constant volume, m_a and m_s are the masses, T_a and T_{ste} are the temperatures, R_a and R_{ste} are specific gas constants of the air and the steam in cylinder at the beginning of the compression. R_{a},R_{ste},$C_{\mathrm{v,a}}$ and $C_{\mathrm{v,s}}$ are 0.287, 0.4615, 0.718 and 1.4108 kJ/kg K, respectively. Other values are changing with respect to cycle condition. The expression of total friction mean effective pressure (tfmep) is stated as: [41]

$$tfmep = C_3 + 48\left(\frac{NR}{1000}\right) + 0.4\overline{S}_P^2 \tag{35}$$

where $C_3 = 75$ kPa, NR is revolution per minute.

4. Results and discussion

In order to investigate the effects of applying the Miller cycle on the performance and NO emissions of the steam injected Diesel engine, Late Intake Valve Closing (LIVC) Miller Cycled Diesel Engine has been modeled by using two-zone combustion model. While the earlier theoretical works related with internal combustion engines are focused on finite time thermodynamics theory and air standard Cycle models, the experimental studies do not contain a comprehensive theoretical basis on diesel combustion [1,5–8,10,12]. As apart from the earlier studies, this study considers the effects of steam injection on Miller Cycled Diesel engines by using two zone combustion model. The results obtained from the model has been compared with those of conventional Diesel engine, steam injected Diesel engine and Miller Cycled Diesel engine. Steam injection ratio is defined as a mass percentage of fuel injected into the cylinder per cycle. 20% steam injection mass ratio (S20) is used in the numerical analysis. Four engine modes have been modeled. These are Standard Diesel Engine (STD), Miller Cycled Diesel Engine (M), Steam Injected Diesel Engine (S20), Steam Injected Miller Cycled Diesel Engine (M-S20). The engine parameters used in the model are given in Table 1.

Fig. 1 illustrates the change of pressure versus crank angle. As seen on the plot, the peak pressure of the Miller Cycled Diesel Engine (M) is lower than the Diesel Engine (STD). The engines with steam injection have higher peak pressures comparing with those of the Miller Cycled Diesel Engine and the Diesel engine.

The change of burned gas temperatures of the Diesel Engine and Miller Cycled Diesel Engine with respect to steam injection and crank angle is shown in Fig. 2. The Miller Cycled Diesel Engine has lower burned gas temperature than the Diesel Engine. Steam injection reduces the burned gas temperature of the cycles. In the figure, one can see that steam injection on Miller Cycled Diesel minimize the gas temperature more than that of the miller cycle.

Heat release rate graph is shown in Fig. 3. The Miller Cycled Diesel Engine with steam has minimum peak heat release rate. Applying the miller cycle reduces peak heat release rates more than applying the steam injection to the diesel engine.

As seen in Fig. 4, steam injection causes to decrease ignition delay but applying the Miller cycle to Diesel Engine leads to increase the ignition delay. Steam injected Miller cycled diesel engine has longer ignition delay than diesel engine cycles. However, when steam injection

Table 1
Engine specifications.

Fuel	Diesel ($C_{14.4}H_{24.9}$)
Speed range	1200–2400 rpm
B/S	10.8/10 cm
R	17
C	0.8
θ_{si}	−35
θ_{di}	8
n	2
RGF	0.1
ϕ	0.77
P_1	1 bar
T_1	300 K
T_{ste}	406 K
T_{w}	400 K

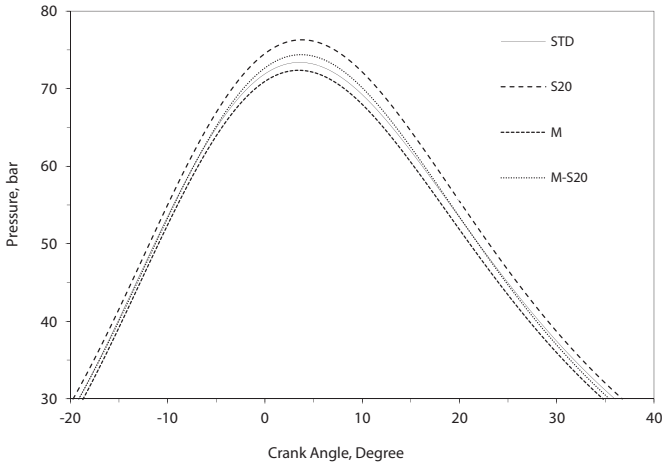

Fig. 1. Comparison of the pressures for various engine modes with respect to crank angle at 2200 rpm.

is applied to Miller Cycled Diesel Engine, ignition delay considerably decreases comparing with that of Miller Cycled Diesel engine without steam injection.

Fig. 5 shows the effective powers of the Diesel Engine and Miller Cycled Diesel Engine with respect to engine speed. The effective power increases with steam injection and decreases with Miller cycle application. The peak effective power is obtained with the steam injected Diesel Engine. When the engine is operated without steam injection, the maximum power of Miller Cycled Diesel Engine is found 11.32 kW at 2200 rpm. The maximum reduction rate in the effective power is −6.04%. At the condition of steam rate of 20% and 2400 rpm engine speed, the maximum effective power is obtained as 11.6 kW. The power was decreased −6.013%. The minimum effective power is 6.48 kW, which is measured at 1200 RPM in the standard condition. The power was decreased −5.27%.

The reason of power reduction is that lesser air entering into the cylinder in the modes of Miller Cycle and steam injected Miller Cycled Diesel engines as inlet valve closes later compared to those of the other two modes. The power reduction can be eliminated or minimized by supercharging and optimizing the injection timing, coordinately.

Fig. 6 illustrates the effective efficiencies of the Diesel Engine and Miller Cycled Diesel Engine with respect to steam injection ratio and engine speed. While the effective efficiency increases at 1200–2000 rpm range, on the contrary, a reduction is seen in the effective efficiency after 2000 rpm. The engines with the steam injection have higher effective efficiencies in all conditions. The Miller Cycled Diesel Engine with steam injection has maximum effective efficiency until 2000 rpm. The maximum effective efficiency of Miller Cycled Diesel Engine is 29.745% at 1600 RPM under the standard condition. There is 0.44% increase in the effective efficiency.

Fig. 7 shows the NO emission of the Diesel Engine and Miller Cycled Diesel Engine with respect to engine speed. There is a steady reduction in NO emission released from the Miller Cycled Diesel Engine with respect to engine speed. Under the standard condition, the minimum NO of Miller Cycled Diesel Engine is 659 ppm and at 1600 rpm, the reduction in NO emission is −26.25%. The minimum NO released is 490 ppm at the condition of steam ratio of 20% and 1200 rpm engine speed. NO emissions decreased −28.98%. At the condition of steam ratio of 20% and 2200 rpm engine speed, NO is 536 ppm, when it is compared to standard condition, the decrease in NO is reached to −36.75%.

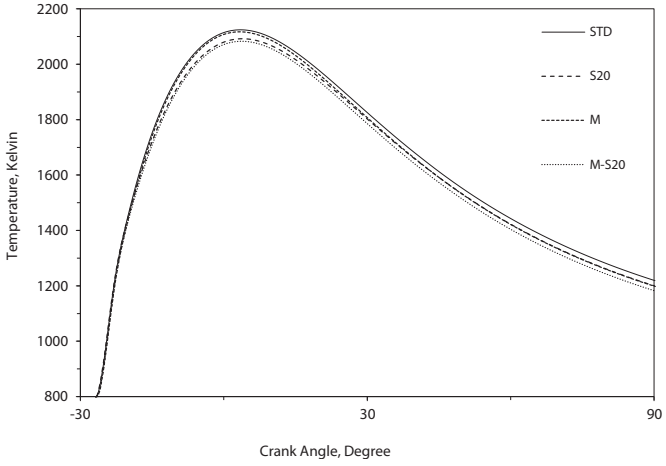

Fig. 2. Comparison of the burned gas temperatures for various engine modes with respect to crank angle at 2200 rpm.

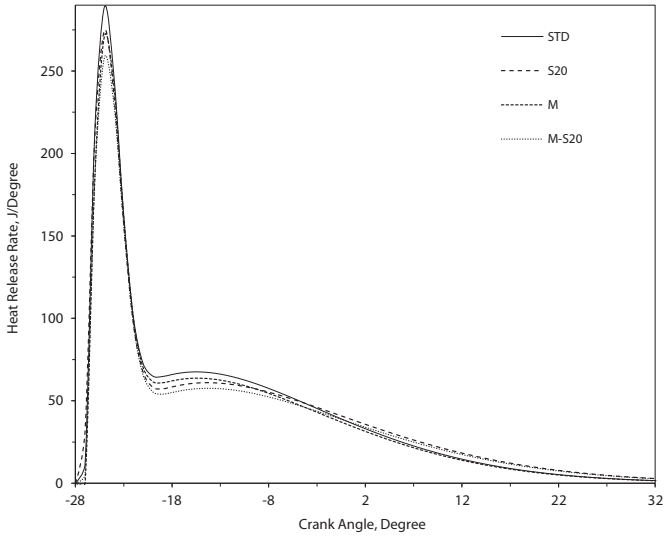

Fig. 3. Comparison of the heat release rates for various engine modes with respect to crank angle at 2200 rpm.

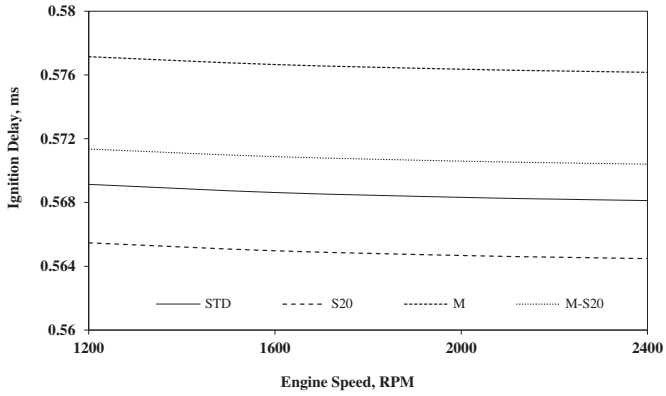

Fig. 4. Comparison of ignition delays for various engine modes with respect to engine speed.

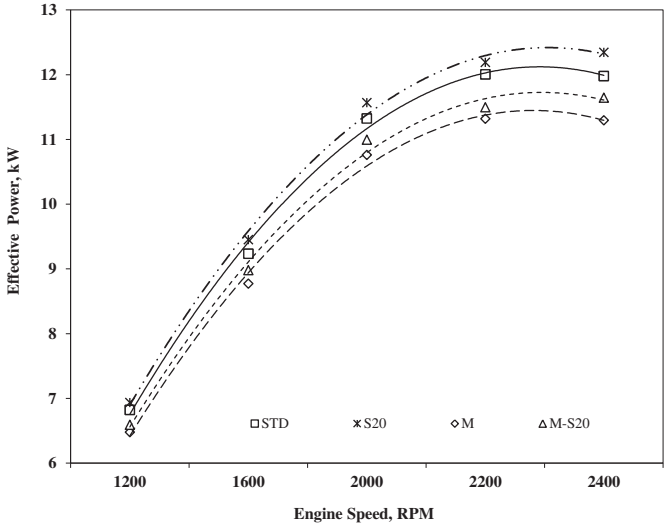

Fig. 5. Comparison of effective powers for various engine modes with respect to engine speed.

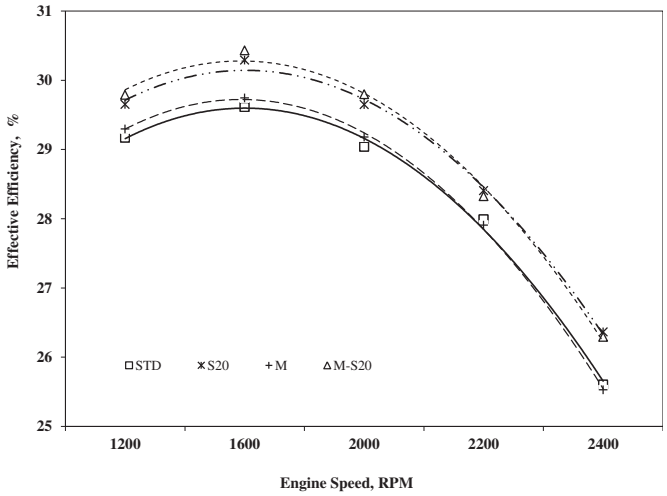

Fig. 6. Comparison of the effective efficiency for various engine modes with respect to engine speed.

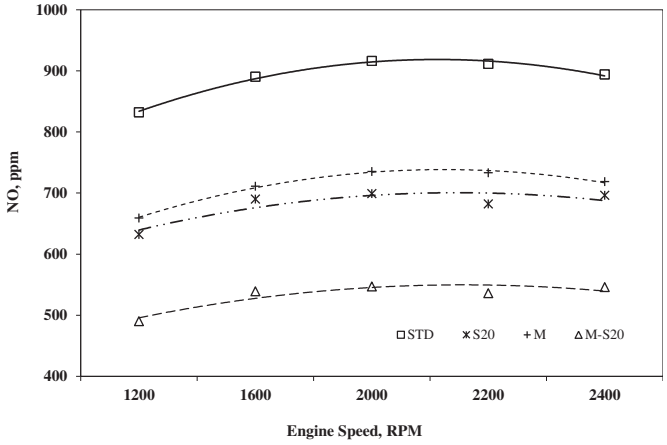

Fig. 7. Comparison of the NO emissions for various engine modes with respect to engine speed.

5. Conclusion

In this study, Late Intake Valve Closing (LIVC) Miller Cycled Diesel Engine has been modeled by using two-zone combustion model. The results have been compared to those of three modes of engines. The study showed that while Steam Injected Miller Cycled Diesel Engine has given the best results in terms of effective efficiency and NO emissions, the effective power increased only compared to that of Miller Cycle. When the Miller cycle is applied to the engine, NO emissions decreased in the all conditions, the effective efficiency is also increased at 1200–2000 rpm range, but there is a reduction in the effective efficiency after 2000 rpm. The loss in the power can be recovered by using supercharging and injection timing optimization.

It can be said that the integrated engine model investigated is more environmentally friendly in all conditions but this data must be verified with experimental data. This study may be used as an approximation in the engineering applications; it could be a leading study for the real-engine designers in the optimization between the effective efficiency, effective power and NO emission.

Acknowledgment

This work has been supported by The Scientific and Technological Research Council of Turkey (TUBITAK, Project No: 111M065) and Yildiz Technical University with the Project No. 2011-10-01-KAP03. This study is a part of PhD thesis of the first author and it was presented and discussed in the 12. International Combustion Symposium.

References

[1] Y. Wang, S. Zeng, J. Huang, Y. He, X. Huang, L. Lin, Proc. IMechE A J. Power Energy 219 (2005) 631–638.
[2] R. Mikalsen, Y.D. Wang, A.P. Roskilly, Appl. Energy 86 (2009) 922–927.
[3] Y. Wang, L. Lin, A.P. Roskilly, S. Zeng, J. Huang, Y. He, Appl. Therm. Eng. 27 (2007) 1779–1789.
[4] Y. Ge, L. Chen, F. Sun, C. Wu, Appl. Energy 81 (2005) 397–408.
[5] Y. Ge, L. Chen, F. Sun, C. Wu, Int. Commun. Heat Mass Trans. 32 (2005) 1045–1056.
[6] A. Al-Sarkhi, J.O. Jaber, S.D. Probert, Appl. Energy 83 (2006) 343–351.

[7] J.C. Lin, S.S. Hou, Int. J. Therm. Sci. 47 (2008) 182–191.
[8] A. Al-Sarkhi, I. Al-Hinti, E. Abu-Nada, B. Akash, Int. Commun. Heat Mass Trans. 34 (2007) 897–906.
[9] C. Wu, P.V. Puzinauskas, J.S. Tsai, Appl. Therm. Eng. 23 (2003) 511–521.
[10] U. Kesgin, Int. J. Eng. Res. 29 (2005) 189–216.
[11] K. Uzuneanu, T. Panait, Termotechnica (2007) 32–34.
[12] Y. Zhao, J. Chen, Appl. Therm. Eng. 27 (2007) 2051–2058.
[13] G. Gonca, H.K. Kayadelen, A. Safa, B. Sahin, A. Parlak, Y. Ust, in: Proc. 1st Int. Conf. on "Naval Architecture and Maritime", Turkey, Istanbul, October 2011. Paper 17. 2.
[14] G. Gonca, Investigation of the Effect of Steam Injection on Performance and Emissions in a Turbocharged Diesel Engine Running with the Miller Cycle, PhD. Thesis, 2013.
[15] G. Gonca, B. Sahin, Y. Ust, A. Parlak, Arab. J. Sci. Eng. 38 (2013) 383–393.
[16] G. Gonca, B. Sahin, Y. Ust, Energy 5 (2013) 285–290.
[17] J.P. Melo, SAE 1 (1999) 836.
[18] M. Christensen, B. Johansson, SAE 1 (1999) 182.
[19] K.P. Duffy, A.M. Mellor, SAE 2 (1998) 460.
[20] M.A. Psota, W.L. Easley, T.H. Fort, A.M. Mellor, SAE Trans. J. Eng. 106 (1997) 1835–1843.
[21] S. Kohketsu, K. Mori, K. Sakai, SAE (1996) 0033.
[22] Y. Yoshimoto, M. Tsukaara, T. Kuramoto, SAE (1996) 2022.
[23] F. Bedford, C. Rutland, P. Dittrich, A. Raab, F. Wireleit, SAE 01 (2000) 2938.
[24] O. Armas, R. Ballesteros, F.J. Martos, J.R. Agudelo, Fuel 84 (2005) 1011–1018.
[25] M. Abu-Zaid, Energy Convers. Manage 45 (2004) 697–705.
[26] A. Sarvi, P. Kilpinen, R. Zevenhoven, Fuel Pro Tech. 90 (2009) 222–231.
[27] V. Ayhan, Investigation of the Effects of Steam Injection into the Diesel Engine on NO_x and PM Emissions, Sakarya University, 2009. PhD. Thesis.
[28] A. Parlak, V. Ayhan, Y. Ust, B. Sahin, I. Cesur, B. Boru, G. Kokkulunk, J. Energ. Inst. 85 (2012) 135–139.
[29] G. Kokkulunk, G. Gonca, V. Ayhan, I. Cesur, A. Parlak, Appl. Therm. Eng. 54 (2013) 161–170.
[30] I. Cesur, A. Parlak, V. Ayhan, B. Boru, G. Gonca, Appl. Therm. Eng. 55 (2013) 61–68.
[31] G. Gonca, Energy Convers. Manage 77 (2014) 450–457.
[32] A. Parlak, V. Ayhan, I. Cesur, G. Kokkulunk, Fuel Process. Technol. 116 (2013) 101–109.
[33] G. Gonca, B. Sahin, Y. Ust, A. Parlak, J. Renew. Sustain. Energy 5 (023119) (2013) 1–13.
[34] R. Ferguson, Internal Combustion Engines-Applied Thermodynamics, John Wiley & Sons, New York, 1986.
[35] A. Safa, Process and Emission Modeling in the Internal Combustion Engines, Ph.D. Thesis, Yildiz Technical University Graduate School of Natural and Appl Sci, 2006. Istanbul (in Turkish).
[36] G.F. Hohenberg, SAE (1979) 0825.
[37] G. Sitkei, Kraftstoffaufbereitung und Verbrennung bei Dieselmotoren, Springer Verlag, Berlin, 1964.
[38] N. Miyamoto, T. Chikahisa, T. Murayama, R. Sawyer, SAE (1985) 0107.
[39] G.L. Borman, K.W. Ragland, Combustion Engineering, McGraw-Hill Book Company, Boston, 1998.
[40] C. Olikara, G.A. Borman, SAE (1975) 0468.
[41] J.B. Heywood, in: Internal Combustion Engines Fundamentals, McGraw Hill Book Company, New York, 1989.